

Periodic magnetic focusing of sheet electron beams*

J. H. Booske,[†] M. A. Basten, and A. H. Kumbasar

Electrical and Computer Engineering, University of Wisconsin—Madison, Madison, Wisconsin 53706

T. M. Antonsen, Jr., S. W. Bidwell, Y. Carmel, W. W. Destler, V. L. Granatstein,
and D. J. Radack

Laboratory for Plasma Research, University of Maryland, College Park, Maryland 20742-3511

(Received 3 November 1993; accepted 14 December 1993)

Sheet electron beams focused by periodically cusped magnetic (PCM) fields are stable against low-frequency velocity-shear instabilities (such as the diocotron mode). This is in contrast to the more familiar unstable behavior in uniform solenoidal magnetic fields. A period-averaged analytic model shows that a PCM-focused beam is stabilized by ponderomotive forces for short PCM periods. Numerical particle simulations for a semi-infinite sheet beam verify this prediction and also indicate diocotron stability for long PCM periods is less constraining than providing for space-charge confinement and trajectory stability in the PCM focusing system. In this article the issue of beam matching and side focusing for sheet beams of finite width is also discussed. A review of past and present theoretical and experimental investigations of sheet-beam transport is presented.

I. INTRODUCTION

A strong motivation for the use of thin ribbon or sheet electron beams in coherent radiation sources or accelerators derives from the ability to transport large currents at reduced current density through thin clearance spaces or in close proximity to walls or structures. This feature is a result of the opportunity to add current to the beam at constant current density by increasing one wide transverse beam dimension, while keeping the other beam transverse dimension very small. A historically strong disincentive to using sheet electron beams in the above-mentioned applications is their known susceptibility to the disruptive diocotron instability occurring in the presence of a uniform solenoidal magnetic (focusing) field.

Recent research appears to have identified a solution to this decades-old problem, paving the way for implementation of sheet beams in both relativistic and nonrelativistic applications. The essence of the solution is to use ponderomotive focusing achieved with one of several configurations of spatially periodic magnetic fields.

In this paper we present an organized review of the physics and recent results of research of periodically focused sheet electron beams, and we describe new results of simulation studies of beam stability and emittance growth.

II. HISTORICAL REVIEW

The advantage of using sheet electron beams for high current applications was first noted over three decades ago.¹ However, around the same time, experiments with both thin annular²⁻⁴ and planar⁴ sheet beams identified a filamentation instability when the beams were propagated parallel to a uniform solenoidal magnetic focusing field. The simplest theoretical model was derived for a very thin, monoenergetic, nonrelativistic, planar sheet beam, and

considered only low-frequency, quasistatic perturbations transverse to the magnetic field axis.⁵ Since then, both the experimental and theoretical details have become considerably more sophisticated, including finite beam thickness, thermal velocity spread, relativistic beam energies, nearby conducting boundaries, ion-space-charge neutralization, off-axis beam placement, intense magnetic field strengths, and nonlinear effects. In all cases, the instability is driven by $\mathbf{E} \times \mathbf{B}$ drift velocity shear. A partial listing of prior work can be found in Refs. 6–11 and references cited therein. Nevertheless, the ubiquitous presence of this breakup or “diocotron” instability in so many circumstances has largely discouraged aggressive research into accelerator and coherent radiation sources based on sheet electron beams.

The first suggestion of periodic magnetic focusing for sheet beams was made by Sturrock.¹ In a preceding companion article, Sturrock theoretically established the principle of periodic focusing of rectilinear beams using a general “Hamilton’s principle” analysis that included both electric and magnetic periodic focusing fields.¹² The subsequent discussion in Ref. 1, however, focused on the application of periodic magnetic focusing. In particular, Ref. 1 advocated the use of periodic *transverse* magnetic fields (henceforth, referred to as “wiggler” fields—a term familiar to the both accelerator and microwave sources communities). In a planar wiggler magnet configuration, the fields near the midplane of the gap are primarily transverse, with a weaker longitudinal component seen only by off-midplane electrons. Recognizing this feature, Sturrock surmised that this configuration was least susceptible to the diocotron disruption associated with longitudinal magnetic fields, as reported by Webster.² As we shall discuss below, Sturrock’s idea was basically sound, although he need not have been so concerned with longitudinal field components.

The first experimental study of periodic magnetic focusing of sheet electron beams was conducted by Dryden.¹³

*Paper 2I2, Bull. Am. Phys. Soc. 38, 1901 (1993).

[†]Invited speaker.

These early experiments confirmed the basic concept of periodic magnetic focusing (used a “wiggler” configuration), but the results would have to be considered inconclusive regarding beam stability, owing to significant wall interception losses. Possible reasons cited for the large interception currents included significant emittance in the injected beam, as well as significant period-to-period field errors in the magnet array. However, the precise explanation was not identified at the time. Furthermore, theoretical analyses of beam “stability” in both Refs. 12 and 13 only considered the stability of single-particle trajectories^{12,13} or gross beam displacement,¹³ rather than overall stability of the beam to diocotron-like kink modes. Thus, the stability of sheet beams to diocotron modes in periodic magnetic focusing has remained an open issue until very recently.

III. PERIODIC MAGNETIC FOCUSING OF SHEET ELECTRON BEAMS—ANALYTIC THEORY

A. Equations of motion

Periodic magnetic focusing of rectilinear electron beams is the result of a ponderomotive force effect that arises from coupled $\mathbf{v} \times \mathbf{B}$ forces in two-component periodic magnetic fields. If we assume for the moment that the magnetic field is spatially uniform in the “ x ” dimension (this will represent the “horizontal” or wide transverse dimension of the sheet beam), then we can most compactly describe it in terms of a vector magnetic potential, $\mathbf{B}(y,z) = \nabla \times \mathbf{A}(y,z)$, where $\mathbf{A}(y,z) = A_m(y,z) \hat{x}$. To simplest order, this vector potential of a planar periodic magnet array characterized by spatial period $l_m = 2\pi/k_m$ can be approximated by either the choice

$$A_m(y,z) \approx -(B_0/k_m) \cosh(k_my) \cos(k_mz), \quad (1a)$$

for a “wiggler” field,⁷ or by

$$A_m(y,z) \approx -(B_0/k_m) \sinh(k_my) \cos(k_mz), \quad (1b)$$

for a periodically cusped magnetic (PCM) field.¹⁴ Assuming that $z \approx u_0 t$ (u_0 is a constant) and that $u_0 \gg |y|$, the electron equations of motion for combined magnetic and self-electric forces are

$$\ddot{x} = \frac{q}{m\gamma^3} E_x + \frac{\omega_{cy}(y,z)}{\gamma} u_0, \quad (2a)$$

$$\ddot{y} = \frac{q}{m\gamma^3} E_y - \frac{\omega_{cz}(y,z)}{\gamma} \dot{x}. \quad (2b)$$

In Eqs. (2), we have implicitly incorporated self-magnetic fields through a $1/\gamma^2$ reduction of the self-electric fields, and have ignored axial bunching effects. The parameter m refers to the rest mass of the particle and $\omega_{cy}(y,z) \equiv qB_y(y,z)/m$ and $\omega_{cz}(y,z) \equiv qB_z(y,z)/m$, where B_y and B_z are obtained by taking the curl of the appropriate choice for A_m in Eqs. (1). The periodic focusing term is identified by ignoring space-charge effects, so that

$$\ddot{x} \approx \frac{\omega_{cy}(y,z)}{\gamma} u_0 \quad (3a)$$

and

$$\ddot{y} \approx -\frac{\omega_{cz}(y,z)}{\gamma} \dot{x}. \quad (3b)$$

We further assume that $k_my \ll 1$ and that y fluctuates on a much slower time scale than x , i.e., $\partial \ln y / \partial t \ll k_mu_0$. Integrating Eq. (3a) over the rapid magnetic field fluctuation time scale yields

$$\dot{x} \approx (\omega_{c0}/\gamma k_m) \cos(k_mu_0 t), \quad (4a)$$

for the wiggler field [Eq. (1a)], and

$$\dot{x} \approx (\omega_{c0}y/\gamma) \cos(k_mu_0 t), \quad (4b)$$

for the PCM field [Eq. (1b)], where $\omega_{c0} \equiv qB_0/m$. Substituting these expressions into Eq. (3b) yields

$$\ddot{y} = -\frac{\omega_{c0}^2}{\gamma^2} \cos^2(k_mu_0 t) y, \quad (5)$$

for either type of periodic magnetic field—wiggler or PCM. Making one more usage of the assumption $\partial \ln y / \partial t \ll k_mu_0$, one can “period average” Eq. (4b) over the fast-time scale to obtain

$$\ddot{y} \approx -\frac{\langle \omega_{cz} \dot{x} \rangle}{\gamma} = -\frac{\omega_{c0}^2}{2\gamma^2} y. \quad (6)$$

Thus, we can see that the product of two rapidly fluctuating terms— \dot{x} and B_z —yields a ponderomotive focusing force that survives the fast-time average. Space-charge effects can be easily incorporated if we assume that any added dynamics arising from their inclusion occur on slower time scales. Anticipating multiple-time-scale solutions of the form $x(t) = x_f + x_s$, $y(t) = y_f + y_s$ (where the subscripts refer to “fast” and “slow” time scales, respectively), one obtains the slow-time-scale equations of motion:

$$\ddot{x}_s \approx \frac{q}{m\gamma^3} E_x, \quad (7a)$$

$$\ddot{y}_s \approx \frac{q}{m\gamma^3} E_y - \frac{\omega_{c0}^2}{2\gamma^2} y_s. \quad (7b)$$

For an infinitely wide sheet beam with uniform density and zero emittance, $E_y \approx (m/q)\omega_{p0}^2 y$, and hence, the space-charge confinement criterion is obtained from Eq. (7b):

$$\omega_{p0}^2 \ll \frac{\omega_{c0}^2}{2\gamma}, \quad (8)$$

where $\omega_{p0}^2 \equiv n_0 q^2 / m\epsilon_0$ is the usual beam plasma frequency in the beam rest frame and n_0 is the beam particle density.

Equation (8) provides one of two criteria for selecting between wiggler and PCM focusing. The other criterion is obtained by considering the effect of the transverse wiggler fields on the axial velocity z . From Eq. (4a) one obtains

$$z = \sqrt{u_0^2 - \dot{x}_f^2} = \sqrt{u_0^2 - (\omega_{c0}/\gamma k_m)^2 \cos^2(k_mz)}, \quad (9)$$

where we have now relaxed the assumption of a constant axial velocity and have taken u_0 to be the original injection velocity. Except in the case of free electron lasers (FEL's)

or ubitrons, one generally wishes to minimize the axial velocity perturbation, which implies keeping $|\dot{x}_f|^2 \ll u_0^2$. Even in the case of FEL applications, one is constrained to keep $|\dot{x}_f|^2 < u_0^2$, or

$$\frac{\omega_{c0}}{\gamma k_m} < u_0, \quad (10)$$

to avoid complete particle reflection. Substituting for beam density n_0 in terms of beam current density $J_0 = qn_0u_0$, one can combine Eqs. (8) and (10) to obtain an approximate expression, indicating when it is acceptable to consider wiggler fields (as opposed to PCM fields) for periodic magnetic focusing:

$$\sqrt{\frac{2e}{\epsilon_0 mc} \left(\frac{\gamma_0 J_0}{\beta_0} \right)^{1/2}} < \omega_{c0} < \gamma_0 \beta_0 k_m c, \quad (11)$$

where $\beta_0 = u_0/c$ and $\gamma_0 = (1 - \beta_0^2)^{-1/2}$. As an illustration, we consider the case for $l_m = 2$ cm and $J_0 = 100$ A/cm². For these choices, Eq. (11) has no solution below a beam energy of approximately 15 keV. If one applies a more stringent constraint to minimize the axial energy perturbation—e.g., $|\dot{x}_f|^2 < u_0^2/10$ —then the right-hand side of Eq. (11) is reduced accordingly, and the inequality fails to have a solution below a beam energy of approximately 100 keV. In either case, Eq. (11) indicates that low voltage beams require PCM rather than wiggler fields for periodic focusing.

B. Stabilization

In a uniform solenoidal field, e.g., $\mathbf{B} = B_0 \hat{z}$, Eqs. (2a) and (2b) are replaced by

$$\ddot{x} = (qE_x/m\gamma^3) + (\omega_{c0}/\gamma)\dot{y}, \quad (12a)$$

$$\ddot{y} = (qE_y/m\gamma^3) - (\omega_{c0}/\gamma)\dot{x}. \quad (12b)$$

Equations (12) are unstable to low-frequency kink-like diocotron modes of the sort $e^{i(kx - \omega t)}$. In the limit of a thin beam ($k\delta \ll 1$, where δ is the beam thickness), the space charge fields have quasistatic solutions of the form^{5,14} $E_x \approx -(m/2q)\omega_{p0}^2 k \delta x_s$ and $E_y \approx -(m/2q)\omega_{p0}^2 k \delta y_s$, and the perturbations obey the dispersion relation

$$\omega \approx \pm i \frac{\omega_{p0}^2 k \delta}{2\gamma^2 \omega_{c0}}, \quad (13)$$

i.e., purely growing modes. In contrast, Eqs. (7) are stable against these low-frequency perturbations.^{14,15} As a rough guideline, one can expect to achieve stabilization (to diocotron modes) of the sheet beam in periodic magnetic focusing, provided the magnetic field fluctuation frequency $k_m u_0$ is larger than the growth rate given in Eq. (13):

$$k_m u_0 > \frac{\pi \omega_{p0}^2 \delta}{\gamma^2 \omega_c w}, \quad (14)$$

where w is the beamwidth and we have taken the largest value of instability wave number as $k = 2\pi/w$.

For PCM-focused sheet beams, one applies Eq. (14) directly, substituting $\omega_c \sim \omega_{c0}$, the peak magnetic field. Note that PCM focusing is also inherently more immune

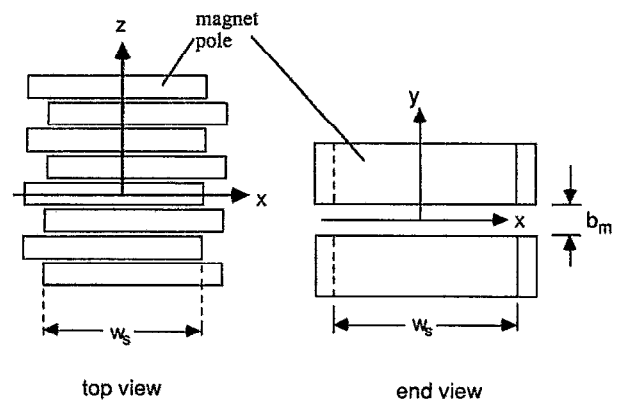


FIG. 1. Schematic of the offset-pole-piece wiggler (or PCM) configuration.

to high-frequency FEL-like electromagnetic instabilities than wiggler focusing due to a significantly lower “wiggling” or quiver velocity amplitude. Specifically, the ratio of quiver energy between PCM and wiggler focusing scales as¹⁴

$$(v_{x,RMS}^2)_{PCM} / (v_{x,RMS}^2)_{wiggler} \sim k_m^2 \delta^2 / 4. \quad (15)$$

In the case of wiggler focusing, only the off-midplane electrons see a nonzero component of longitudinal magnetic field, and this is typically small—of the order $B_z \sim B_0 k_m \delta / 2$. Hence, for wiggler focused sheet beams, Eq. (14) would be of the order:

$$k_m u_0 > \frac{\omega_{p0}^2 l_m}{\gamma^2 \omega_{c0} w}, \quad (16)$$

a requirement favoring wide beams and short magnet periods. Note that the velocity shear in wiggler-focused sheet beams is reduced over that for PCM-focused sheet beams, since electrons on the top and bottom of the beam drift in the same direction, owing to the reversed polarity of B_z on either side of the wiggler (and beam) midplane. Hence Eq. (16) can be considered a conservative estimate.

C. Side focusing

So far, the entire discussion has concentrated on planar periodic magnet arrays with no field variations in the horizontal or “x” dimension. As a result, Eq. (7a) is conspicuously missing a focusing force term that will ensure confinement against space charge expansion in the x direction. There are several options for providing such “side focusing.” With wiggler magnets, one can consider either pole-face profiling¹⁶ or canting. For PCM focusing, one can consider enclosing the sides with pole-face material, in a manner that is topologically equivalent to PPM stacks on conventional (round beam) traveling-wave tubes.¹⁴ However, for both wiggler and PCM focusing, there appears to be an attractive alternative realized by horizontally offset pole pieces.^{14,17,18} The configuration is illustrated for a wiggler magnet array in Fig. 1.

Offset-pole side focusing is based on the principle that after period averaging the dynamics, beam edge electrons

experience a nonzero vertical field component (B_y) of constant polarity. As a result, they experience a constant, inward-deflecting, $u_0 B_y$ force. An approximate analytical model for the fields of a periodic magnet array with offset-pole faces has been derived.¹⁴ From that derivation, one can obtain an approximate expression for the period-averaged side-focusing force as

$$\ddot{x}|_{\text{side focusing}} \approx \frac{u_0 \omega_{c0}}{2\pi v \gamma} \left[\tan^{-1} \left(\frac{w_s/2 + x}{(y - b_m/2)} \right) - \tan^{-1} \left(\frac{w_s/2 - x}{|y - b_m/2|} \right) \right], \quad (17)$$

where $x = \pm w_s/2$ indicates where the beginning of the magnet horizontal offset and b_m is the magnet gap, as indicated in Fig. 1.

Offset-pole side focusing has several advantages. First, it is relatively straightforward to configure and does not require very precise machining of pole face curvature. Second, the amount of focusing force realized by this technique is quite substantial, and is probably adequate for almost any sheet beam application.¹⁴ Third, this configuration with its open-sided topology provides the maximum possible clearance and access to the beam channel. This provides an important feature relevant to input and output radiation coupling for coherent radiation source applications.^{14,17}

IV. EXPERIMENTAL STUDIES WITH WIGGLER-FOCUSED RELATIVISTIC SHEET ELECTRON BEAMS—THE LOW SPACE-CHARGE LIMIT

A. Theoretical predictions for beam focusing and stability

Since 1987, a research program has been in place at the University of Maryland to develop high average power (~ 1 MW) millimeter-wave sources for fusion plasma heating. The high average radiation power requirement implies high average beam power, which, in turn, places severe emphasis on eliminating sources of wall interception current. This concern led to a proposal for a free electron laser source,^{17,19,20} employing a sheet electron beam propagating in the narrow gap of a planar wiggler magnet. The choice of a wiggler magnet exploited the simultaneous provision of both a focusing method as well as a source for inducing coherent gain—i.e., the “lasing” mechanism.

The extreme emphasis on beam propagation with negligibly small interception currents has led to a FEL design with very stiff (low space-charge) beam parameters (e.g., high voltage and modest current density). A recent design²¹ specifies a beam voltage of 0.86 MV and a current density of 100 A/cm². Based on Eq. (8), space-charge focusing requires $B_0 > 1.1$ kG—a relatively modest requirement given the state of the art in wiggler magnet design. In fact, a peak wiggler field of 7.0 kG has been proposed as an ultimate design goal.²¹

Equation (16) can be used to specify a maximum allowable magnet period l_m to suppress diocotron instability. Using the same design parameters quoted above and in-

cluding a specified¹⁹ sheet beam width of 3.0 cm, one obtains $l_m < 80$ cm for stability against diocotron modes. This large number is consistent with the choice of stiff beam parameters, and is easily satisfied by the design specification of $l_m = 1.0$ cm.²¹

So far, the discussion on beam focusing requirements has only considered space charge. However, it is well known that nonzero transverse beam emittance can be of equal importance, since particles with larger transverse momenta will be associated with larger transverse betatron orbit amplitudes. To illustrate with a simplified calculation, we start with the familiar force balance between a linear transverse focusing force and kinetic outward pressure due to finite emittance²² $k_\beta^2 y_{\text{RMS}}^2 \geq \epsilon^2 / 16 y_{\text{RMS}}^3$, where k_β is the wave number of betatron particle orbits. Using Eq. (6), we recast this relation as a limit on the maximum possible beam emittance that can be focused by a set of periodic magnetic focusing parameters:

$$\epsilon_y \leq \frac{\omega_{c0} \delta_{\text{RMS}}^2}{4\sqrt{2}c \sqrt{\gamma^2 - 1}}, \quad (18)$$

where δ_{RMS} is the RMS beam thickness and $\pi\epsilon_y$ is the (unnormalized) RMS beam emittance (in units of length-rad) in the transverse (y) dimension. The 0.86 MV sheet beam FEL design referenced above specifies a beam thickness $\delta_{\text{RMS}} \sim 1.0$ mm. Based on the design specification of a 7.0 kG peak magnetic field amplitude, Eq. (18) implies a maximum RMS transverse emittance of approximately $\epsilon_y \sim 30\pi$ mm mrad.

B. Experimental results on beam focusing and stability

To summarize the section above, theoretically predicted requirements on wiggler field amplitude and spatial period for beam focusing and stabilization are all much less stringent than the requirements imposed by the desired FEL frequency and amplifier gain. In fact, the theory predicts that the confinement behavior of relativistic, low-space-charge sheet electron beams in periodic magnetic fields should be dominated by single-particle-orbit theory. On this basis, one might expect a rather robust beam stability and high transport efficiency. This expectation has been confirmed in a sequence of experiments on wiggler-focused relativistic sheet electron beams.

Initial experiments⁷ conducted with a five-period-long wiggler represented the first feasibility demonstration for wiggler focusing of relativistic sheet electron beams. These early experiments using a 1 cm period wiggler supported the prediction of sheet beam stability by failing to display any significant breakup or filamentation. However, a new challenge was identified, associated with the tendency of the beam to drift in the horizontal dimension. This drift was explained for x -independent wiggler fields by conservation of canonical momentum in the x dimension.⁷ The typical solution to this problem is to use an input taper on the wiggler magnetic field amplitude.¹⁸

A second set of experiments was conducted on a ten-period-long wiggler, which again used a magnet period of

approximately 1 cm.^{17,23} These experiments confirmed the prior measurements, indicating stability against diocotron filamentation. More importantly, they confirmed the theoretical prediction that for confinement of stiff beams, finite beam emittance is more critical than space charge. In particular, these experiments demonstrated that achieving negligibly small wall interception current—i.e., complete sheet beam confinement—is feasible, provided that injected beam emittance is kept very small.^{17,23} The results were consistent with Eq. (18).

Most recently, experiments have demonstrated well-confined sheet electron beam transport through a 56-period-long wiggler channel with a 1.0 cm spatial magnet period.^{18,21} These experiments have included studies of the effects of various input field tapers, variable beamwidths, and offset-pole side focusing on sheet beam confinement. Due to the considerable length of the transport system, these measurements may be considered the first definitive experimental test of the offset-pole side-focusing concept. The results indicated nearly 100% complete beam transmission for sheet beamwidths up to 20 mm, provided the wiggler entrance fields were carefully tapered. Less optimum entrance field tapers yielded significantly reduced beam current transport efficiencies as a result of the horizontal drift effect mentioned earlier.¹⁸ Because of the method of beam formation, sheet beams wider than 20 mm were characterized by significantly larger values of emittance ϵ_x in the horizontal dimension. Hence, the experimental results suggest that offset-pole side focusing is considerably less effective for beams with large emittance in the wide transverse dimension. Understanding this behavior and the detailed physics of offset-pole side focusing is an important topic for future study.

To summarize this work, it has been theoretically and experimentally established that relativistic, low-voltage sheet electron beams focused by periodic magnetic fields are robustly stable to disruptive instabilities (e.g., diocotron). More importantly, these stiff beams exhibit highly predictable behavior that is well described by single-particle-orbit theory. The implication of this last point for the feasibility of the high-power FEL designs²¹ is very favorable, in that *a priori* predictions of negligible interception currents for carefully chosen FEL designs can be accepted with a high degree of confidence.

V. ANALYTIC AND NUMERICAL STUDIES OF PCM-FOCUSED NONRELATIVISTIC SHEET BEAMS—THE SPACE-CHARGE DOMINATED REGIME

The University of Maryland research described above has broken new ground in the search for a stable method of confining sheet electron beams. However, in a physics sense, the context of this work is narrow because the stiff, relativistic energy beam parameters were intentionally chosen to be in a “single-particle-orbit regime,” where space charge effects are minimal. Hence, it may not be surprising that the experiments indicated a robust stability to the disruptive diocotron mode—a space-charge-induced phenomenon.

To investigate the behavior of *space-charge-dominated* sheet beams in periodic magnetic focusing, a research program has been established at the University of Wisconsin to study PCM focusing of nonrelativistic sheet electron beams. The concentration on lower beam voltages necessitates the use of PCM focusing, as previously discussed. However, the use of lower beam voltages also places a greater emphasis on space charge effects than in the case of the stiff relativistic beams. For example, it is expected that low voltage beams in PCM focusing should be more susceptible to diocotron-like disruption (than wiggler-focused relativistic sheet beams) if the magnet period is too large. This point was indirectly made in an earlier analysis by Dohler,²⁴ and we will explore it in greater detail below. In contrast to wiggler focusing, however, PCM focusing is less susceptible to high-frequency electromagnetic instabilities, and is not susceptible to horizontal drift.

Recent analyses¹⁴ have made a start on analyzing the specific physics of offset-pole side focusing, and the more general issue of two-dimensional beam matching (i.e., a balance between space charge and focusing forces) in PCM-focusing channels. In general, the analytic fluid theory predicted that two-dimensional (2-D) laminar beam equilibria cannot be found for sheet beams with rectangular cross sections (i.e., constant thickness across the entire beamwidth), since the beam edges always end up being overfocused for matched conditions near the horizontal center of the beam. However, elongated elliptical cross section sheet beams were shown to have properties consistent with achieving a matched beam.

Recently, a more detailed understanding and appreciation of the physics of PCM-focused sheet beams have been obtained via particle-in-cell (PIC) numerical simulations. Although the PIC code used is only “2½-D” (two dimensional in spatial coordinates, three dimensional in momentum coordinates), we have successfully simulated the third spatial degree of freedom (z axis) by transforming into the time domain.¹⁵ A dramatic demonstration of how periodic focusing can ponderomotively stabilize sheet beams against diocotron modes is exhibited in Figs. 2 and 3.

Figure 2 displays the unstable behavior of a sheet beam immersed in a uniform solenoidal magnetic field. The initial beam configuration in Fig. 2(a) is “seeded” by a density bunch of excess charge within the indicated region at the center of the beam (in an experiment, such bunches will grow from “noise-level” inhomogeneities in the beam density distribution). The vortex formation driven by the $\mathbf{E} \times \mathbf{B}$ velocity shear is clearly visible. By the end of the simulation run, diocotron filamentation is evident. The initial parameters for this example included a 0.07 T uniform magnetic field (in the z dimension), $u_0 = 5.9 \times 10^7$ m/s (corresponds to 10 keV), a beam thickness $\delta = 2$ mm, and a background beam charge density of $\rho_0 = 2.1 \times 10^{-3}$ C/m³. The density of the “seed” charge bunch in the center of the beam was 60% greater than the background charge density. The left and right boundaries of each frame represent symmetry planes, and are spaced a distance of 10 mm apart. The simulated instability’s growth rate is in qualitative agreement with the approxi-

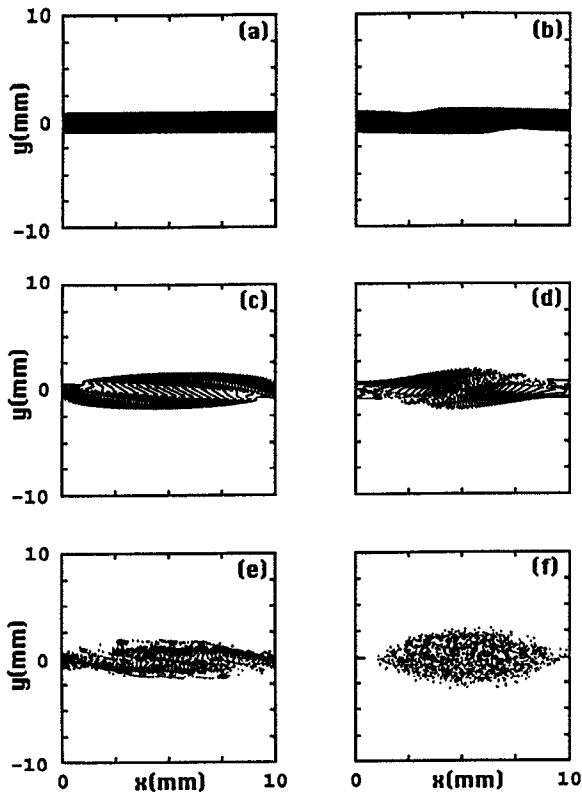


FIG. 2. Evolution of a diocotron instability for a sheet electron beam with an initial density bunch immersed in a uniform axial magnetic field of magnitude B_0 . The magnetic field axis points into the page. The initial conditions were $B_0=0.07$ T, $\rho_{\max}=3.3\times 10^{-3}$ C/m³, $\rho_{\max}/\rho_{\min}=1.6$, $\Delta=\delta=2.0$ mm, $u_0=5.9\times 10^7$ m/s, and the horizontal width of the simulation frame is 10.0 mm (a) $t=0.0$ ns, (b) $t=0.5$ ns, (c) $t=1.4$ ns, (d) $t=2.8$ ns, (e) 4.6 ns, and (f) $t=11.5$ ns.

mate prediction of a 0.5 ns e -folding time obtained from Eq. (13) and the specified parameters.

Results obtained by repeating the above simulation with PCM-like fields are displayed in Fig. 3. For this case, the initial beam conditions were identical with those of Fig. 2. The magnetic field parameters were chosen to simulate a PCM field with a peak amplitude of 0.07 T and a spatial magnet period $l=3.8$ mm. There are three distinct features of this particular simulation. First the gross velocity-shear (diocotron) instability and filamentation observed in Fig. 2 is absent, confirming the analytic predictions. Second, the beam thickness fluctuates in time, due to a ponderomotive focusing force that initially exceeds the beam space-charge forces. This effect is discussed in greater detail elsewhere.¹⁵ Finally, a significant beam “heating” or transverse emittance growth is evident from the trajectory mixing and the slight halo production of Fig. 3. This effect is primarily due to the initially overfocused beam conditions and is driven by localized electrostatic field fluctuations within the beam.^{22,25}

We have also begun to explore the effect of longer magnet periods on beam confinement and stability. For a current density of 12.2 A/cm², magnetic field amplitude $B_0=0.7$ kG, drift velocity $\beta_z=0.2$, and a beam energy of 10 keV, the simulations indicate that the beam is confined

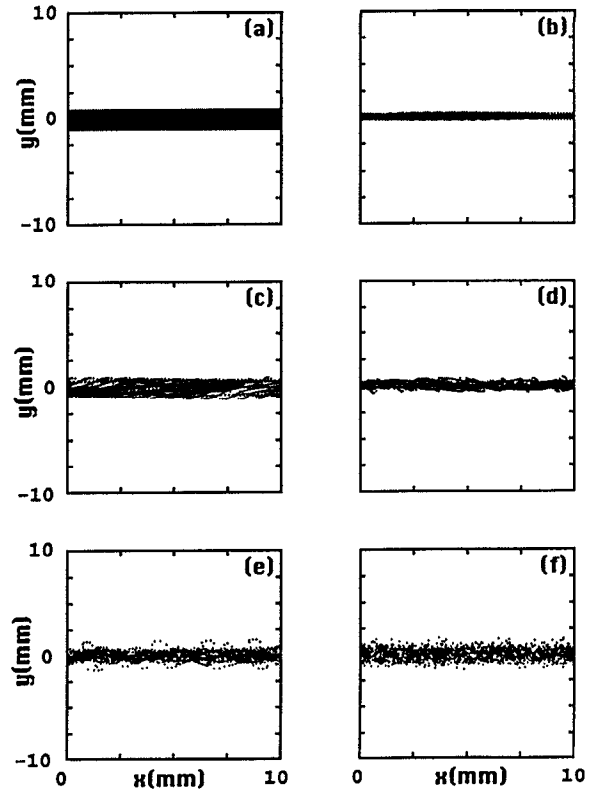


FIG. 3. Simulation demonstrating stabilization of diocotron instability by ponderomotive focusing with rapidly oscillating magnetic fields. Initial conditions for the electron beam were the same as those for Fig. 2. Parameters for the time-harmonic magnetic field included a peak amplitude $B_0=0.07$ T, a magnetic fluctuation frequency $\omega_B=1.0\times 10^{11}$ s⁻¹, and a transverse gradient scale length of $L^{-1}=1.7$ mm⁻¹. (a) $t=0$ ns, (b) $t=0.5$ ns, (c) $t=0.7$ ns, (d) $t=1.2$ ns, (e) $t=1.8$ ns, and (f) $t=12.4$ ns.

to the transport channel for PCM periods below 37 mm. Figure 4 shows the total particle energy in the system described in Fig. 3 except with $l_m=40$ mm. The sudden drop in system particle energy near 1 ns corresponds to particle loss to the walls of the transport channel.

As l_m increases, the separation of particle motion into “fast” and “slow” time scales in the analytic theory of the previous sections becomes inadequate. A semianalytic model was developed, which involves numerically integrating the equations of motion for the beam envelope in the presence of space-charge and the PCM magnetic field model used in the particle simulations. The effects of emittance and emittance growth are neglected for the present. This model demonstrates a transition from periodic, or semiperiodic, confined flow to an exponential expansion of the beam envelope near $l_m=35$ mm, in very good agreement with the particle simulations.

Trajectory stability was examined for a similar magnet configuration (PPM focusing of a cylindrical beam) in Ref. 26 with similar observations. Both Ref. 26 and our semianalytic model predict the existence of regions of trajectory stability for longer magnet periods than those for the unstable region. For the same beam parameters described above, this second stability region occurs for 60 mm $< l_m < 80$ mm. Particle simulations with $l_m=70$ mm

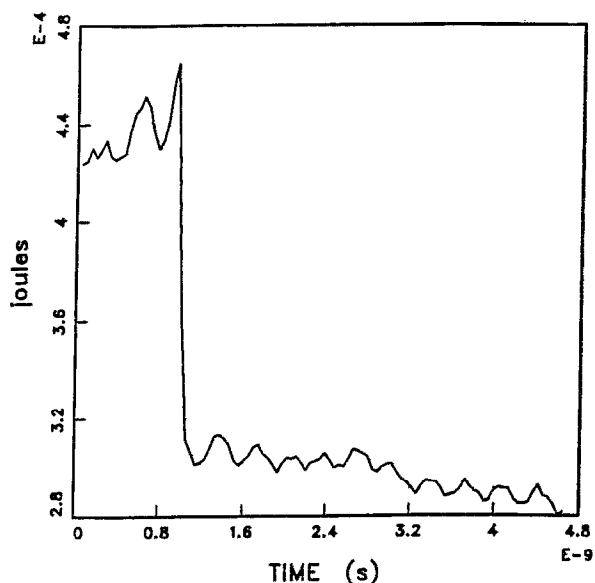


FIG. 4. System particle energy as a function of time with the same beam and magnetic field parameters as in Fig. 3, except with $\omega_B = 9.4 \times 10^{11} \text{ s}^{-1}$ ($I_m = 40 \text{ mm}$). The large drop in total particle energy near 1 ns corresponds to a loss of particles to the walls of the transport channels.

verify the existence of this second trajectory-stable region.

No clear evidence of filamentation associated with velocity-shear instabilities (diocotron growth) was observed in the particle simulations, as the PCM period was lengthened to 70 mm. Rather, it appears as though space-charge confinement and focusing of the beam are the constraining factors in the design of a suitable PCM focusing system for sheet beams. The simulations also indicate that shorter PCM periods provide for lower emittance growth in the initially laminar sheet beam. Emittance growth in the semi-infinite sheet beam, and confinement and matching of a finite width sheet beam are the subjects of current investigation with the particle simulations.

ACKNOWLEDGMENTS

The authors wish to acknowledge helpful discussions with Dr. B. McVey, Dr. G. Scheittrum, Dr. R. True, Dr. J. Scharer, Dr. H. Kirolos, and Mr. Jurianto Joe. The numerical simulation results reported here were obtained using Mission Research Corporation's MAGIC code under the MAGIC User's Group sponsored by the Air Force Office of Scientific Research (AFOSR). The authors acknowledge considerable assistance by Dr. L. Ludeking and Dr. D. Smithe in operating the code.

This work was supported in part by the U.S. Department of Defense Vacuum Electronics Initiative as managed by AFOSR (AFOSR-91-0381), by a National Science Foundation Presidential Young Investigator Award (ECS-9057675), and by the U.S. Department of Energy, Office of Fusion Energy.

- ¹P. A. Sturrock, *J. Electron. Control* **7**, 162 (1959).
- ²H. F. Webster, *J. Appl. Phys.* **26**, 1386 (1955).
- ³R. L. Kyhl and H. F. Webster, *IRE Trans. Electron. Devices* **3**, 172 (1956).
- ⁴C. C. Cutler, *J. Appl. Phys.* **27**, 1028 (1956).
- ⁵O. Buneman, *J. Electron. Control* **3**, 507 (1957).
- ⁶T. M. Antonsen, Jr. and E. Ott, *Phys. Fluids* **18**, 1197 (1975).
- ⁷J. Booske, W. W. Destler, Z. Segalov, D. J. Radack, E. T. Rosenbury, J. Rodgers, T. M. Antonsen, Jr., V. L. Granatstein, and I. D. Mayergoyz, *J. Appl. Phys.* **64**, 6 (1988).
- ⁸K. S. Fine, C. F. Driscoll, and J. H. Malmberg, *Phys. Rev. Lett.* **63**, 2232 (1989).
- ⁹R. C. Davidson, H. W. Chan, C. Chan, and S. Lund, *Rev. Mod. Phys.* **63**, 341 (1991).
- ¹⁰C. A. Kapetanakis, D. A. Hammer, C. D. Striffler, and R. C. Davidson, *Phys. Rev. Lett.* **30**, 1303 (1973).
- ¹¹A. J. Peurrung and J. Fajans, *Phys. Fluids A* **5**, 493 (1993).
- ¹²P. A. Sturrock, *J. Electron. Control* **7**, 153 (1959).
- ¹³V. W. Dryden, Ph.D. dissertation, Department of Electrical Engineering, Stanford University, 1960.
- ¹⁴J. H. Booske, B. D. McVey, and T. M. Antonsen, Jr., *J. Appl. Phys.* **73**, 4140 (1993).
- ¹⁵J. H. Booske, A. H. Kumbasar, and M. A. Basten, *Phys. Rev. Lett.* **71**, 3979 (1993).
- ¹⁶E. T. Scharlemann, *J. Appl. Phys.* **58**, 2154 (1985).
- ¹⁷J. H. Booske, D. J. Radack, T. M. Antonsen, Jr., S. W. Bidwell, Y. Carmel, W. W. Destler, H. P. Freund, V. L. Granatstein, P. E. Latham, B. Levush, I. D. Mayergoyz, and A. Serbeto, *IEEE Trans. Plasma Sci.* **PS-18**, 399 (1990).
- ¹⁸Z.-X. Zhang, V. L. Granatstein, W. W. Destler, S. W. Bidwell, J. Rodgers, S. Cheng, T. M. Antonsen, Jr., B. Levush, and D. J. Radack, *IEEE Trans. Plasma Sci.* **PS-21**, 760 (1993).
- ¹⁹W. W. Destler, V. L. Granatstein, I. D. Mayergoyz, and Z. Segalov, *J. Appl. Phys.* **60**, 521 (1986).
- ²⁰J. H. Booske, S. W. Bidwell, B. Levush, T. M. Antonsen, Jr., and V. L. Granatstein, *J. Appl. Phys.* **69**, 7503 (1991).
- ²¹See National Technical Information Service Document No. PB92-206-168. [S. W. Bidwell, Z. X. Zhang, T. M. Antonsen, Jr., W. W. Destler, V. L. Granatstein, B. Levush, and J. Rodgers, "Development of a high power millimeter wave free-electron laser amplifier," Technical Digest, 9th International Conference on High Power Particle Beams, 25-29 May 1992, Washington, DC, Vol. 3, p. 1728]. Copies may be ordered from NTIS, Springfield, Virginia 22161.
- ²²M. Reiser, *J. Appl. Phys.* **70**, 1919 (1991).
- ²³D. J. Radack, J. H. Booske, Y. Carmel, and W. W. Destler, *Appl. Phys. Lett.* **55**, 2069 (1989).
- ²⁴G. Dohler, *IEEE Trans. Electron Devices* **ED-28**, 602 (1981).
- ²⁵C. L. Bohn, *Phys. Rev. Lett.* **70**, 932 (1993).
- ²⁶J. T. Mendel, C. F. Quate, and W. H. Yocum, *Proc. IRE* **42**, 802 (1954).